Di- and Trinuclear Ruthenium and Osmium Bis(2-pyridyl) Ketone Oximate Derivatives

Javier A. Cabeza,*[a] Ignacio del Río,[a] Víctor Riera,[a] Marta Suárez,[a] Carmen Álvarez-Rúa,[b] Santiago García-Granda,[b] Shih Hsien Chuang,[c] and Jih Ru Hwu*[c]

Keywords: Ruthenium / Osmium / Cluster compounds / Oximes / DNA cleavage

Treatment of $[Ru_3(CO)_{12}]$ with bis(2-pyridyl) ketone oxime (Hdpko) in refluxing THF leads to a separable mixture of $[Ru_3(\mu,\eta^3\text{-dpko-}N,N,O)_2(CO)_8]$ (**1**) and $[Ru_2(\mu,\eta^3\text{-dpko-}N,N,O)_2(CO)_4]$ (**2**). In both complexes, two Ru atoms are doubly bridged by two dpko ligands, which are attached to a Ru atom through the oximate O atom while chelating the other Ru atom through the N atoms of a pyridyl group and the oximate fragment. While the Ru–Ru distance of the bridged edge of complex **1** is very long [3.5388(9) Å], that of complex **2** is very short [2.620(1) Å]. The acetonitrile complexes $[M_3(CO)_{10}(MeCN)_2]$ (M = Ru, Os) react with Hdpko in THF at room temperature to give $[M_3(\mu\text{-H})(\mu,\eta^3\text{-dpko-}N,N,O)(CO)_9]$ [M = Ru (**3**) Os (**4**)], in which the dpko ligand behaves in the same way as in **1** and **2**. The thermal reaction of **3** with Hdpko leads to a mixture of **1** and **2**, while an analogous treatment of complex **4** gives $[Os_3(\mu,\eta^3\text{-dpko-}N,N,O)_2(CO)_8]$ (**5**), which is isostructural with complex **1**. Compounds **1** and **3** are the first examples of ruthenium clusters containing oximate ligands. These oximate complexes display low activity as DNA cleavage agents, requiring high complex concentrations, long incubation times, and the use of UV light as a trigger.

Introduction

Oximes and oximates are attractive ligands because they can interact with metal atoms through either one or both N and O atoms, acting as terminal (monodentate or chelating)[1,2] or, less frequently, as bridging ligands.[3−6] In addition, oximes can remain intact in the coordination sphere of the metals or undergo O−H bond cleavage to afford oximate derivatives.[1−6] In some cases they can also suffer N−OH bond activation to form nitrenium fragments.[2b,2c,3,4] The osmium cluster-promoted O−H vs. N−O bond cleavage of these ligands has been studied.[4] Despite this rich derivative chemistry and the large number of oximate complexes of transition metals known to date,[1−6] it is noteworthy that no ruthenium and only a few osmium[4−6] cluster complexes containing oximate ligands have been reported.

Herein we report the synthesis and structural characterization of triruthenium and triosmium carbonyl clusters derived from bis(2-pyridyl) ketone oxime (Hdpko). We decided to use this oxime because, in addition to its varied coordination possibilities, its chemistry has been little explored.[7]

[a] Departamento de Química Orgánica e Inorgánica, Instituto de Química Organometálica "Enrique Moles", Universidad de Oviedo-CSIC,
33071 Oviedo, Spain
Fax: (internat.) + 34-985/103446
E-mail: jac@sauron.quimica.uniovi.es
[b] Departamento de Química Física y Analítica, Universidad de Oviedo,
33071 Oviedo, Spain
[c] Department of Chemistry, National Tsing Hua University, Hsinchu 30013, Taiwan, Republic of China
E-mail: jrhwu@mx.nthu.edu.tw

Results and Discussion

Synthesis and Structural Characterization of Oximate Complexes

Treatment of $[Ru_3(CO)_{12}]$ with one equivalent of Hdpko, in THF at reflux temperature, gave a complex mixture of compounds containing some ruthenium carbonyl starting material. When two equivalents of Hdpko were used under the same reaction conditions, the novel trinuclear derivative $[Ru_3(\mu,\eta^3\text{-dpko-}N,N,O)_2(CO)_8]$ (**1**) and the dioximate-bridged binuclear complex $[Ru_2(\mu,\eta^3\text{-dpko-}N,N,O)_2(CO)_4]$ (**2**) were obtained as the major reaction products (Scheme 1).

The ^{1}H NMR spectra of both complexes display no signals attributable to hydride ligands, while the aromatic regions reflect, in both cases, the presence of two inequivalent pyridyl groups. Their IR spectra confirm the absence of bridging carbonyl ligands and display no bands in the O−H stretching region, suggesting O−H bond activation.

The trinuclear nature of **1** was clearly indicated by its microanalysis and FAB MS spectrum, which also show the presence of eight CO ligands and the incorporation of two

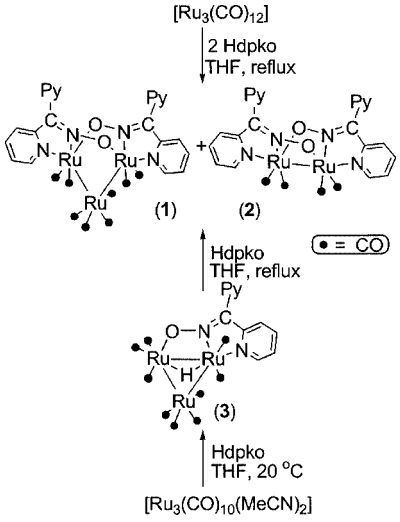

Scheme 1. Synthesis of compounds **1**−**3**

oximate ligands to the cluster shell. The structure of **1** was established by X-ray diffraction methods (Figure 1, Table 1). In addition to eight terminal CO ligands, the complex contains two oximate ligands spanning the same edge of the trimetallic core, in a head-to-tail arrangement, through both the N and O atoms. Each dpko ligand is also attached through a pyridine N-atom to one of the metal atoms of the bridged edge, in such a way that the complex

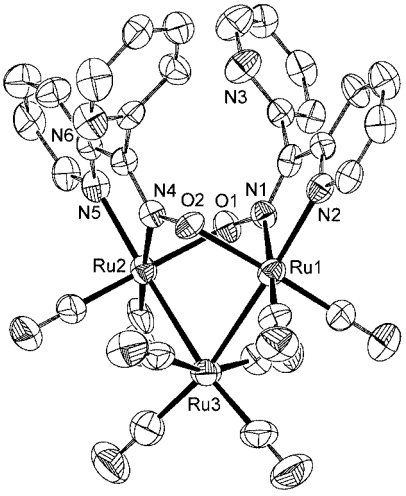

Figure 1. Molecular structure of compound **1** (50% probability level ellipsoids); H atoms omitted for clarity

Table 1. Selected interatomic distances (Å) in complex **1**

Ru(1)−Ru(2)	3.5388(9)	Ru(1)−Ru(3)	2.8137(9)
Ru(2)−Ru(3)	2.8170(9)	Ru(1)−N(1)	2.131(6)
Ru(1)−N(2)	2.173(7)	Ru(2)−N(4)	2.115(6)
Ru(2)−N(5)	2.154(7)	Ru(1)−O(2)	2.131(5)
Ru(2)−O(1)	2.124(5)	N(1)−O(1)	1.350(8)
N(4)−O(2)	1.363(8)		

presents a non-crystallographic twofold axis. Such a symmetry was also indicated by its $^{13}C\{^1H\}$ NMR spectrum, which displays only four carbonyl resonances. The length of the bridged edge [Ru(1)−Ru(2) = 3.5388(9) Å] indicates the absence of a metal−metal bond, as expected for a 50-electron trinuclear cluster.[8]

The $^{13}C\{^1H\}$ NMR spectrum of **2** shows only two signals attributable to terminal carbonyl ligands. Its binuclear character and the incorporation of one dpko ligand per Ru atom were pointed out by its microanalysis and FAB MS. Its structure was confirmed by an X-ray diffraction study (Figure 2, Table 2). The ligand arrangement in compound **2** is analogous to that described above for complex **1**, but the $Ru(CO)_4$ fragment present in **1** is now missing. The Ru(1)−Ru(2) distance in **2**, 2.620(1) Å, is in the range expected for a single metal−metal bond, in accordance with the 34-electron count for the complex.[8] It is noteworthy that the oximate NO fragment is able to bridge two metal atoms which are either close to each other (complex **2**) or very far apart (complex **1**).

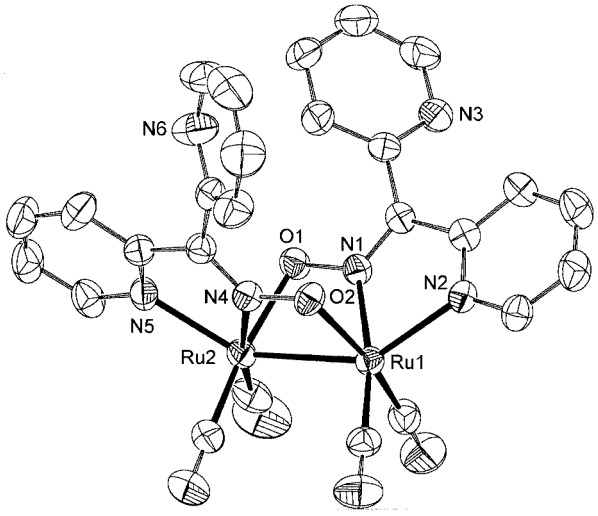

Figure 2. Molecular structure of compound **2** (50% probability level ellipsoids); H atoms omitted for clarity

Table 2. Selected interatomic distances (Å) in complex **2**

Ru(1)−Ru(2)	2.620(1)	Ru(1)−N(1)	2.061(3)
Ru(1)−N(2)	2.209(4)	Ru(2)−N(4)	2.060(4)
Ru(2)−N(5)	2.176(4)	Ru(1)−O(2)	2.162(4)
Ru(2)−O(1)	2.135(3)	N(1)−O(1)	1.341(4)
N(4)−O(2)	1.334(4)		

IR monitoring of the reaction of $[Ru_3(CO)_{12}]$ with Hdpko showed that an intermediate, probably arising from the incorporation of only one equivalent of Hdpko to the cluster, is formed prior to compounds **1** and **2**. Its isolation was not possible under the thermal conditions applied, since it readily reacted with more Hdpko to give **1** and **2** as the two major final products. Fortunately, we managed to isolate this intermediate working at room temperature, using the reactive complex $[Ru_3(CO)_{10}(MeCN)_2]$[9] as starting material. The product was characterized as the novel

trinuclear derivative $[Ru_3(\mu\text{-H})(\mu,\eta^3\text{-dpko-}N,N,O)(CO)_9]$ (**3**; Scheme 1).

The IR spectrum of **3** strongly suggests O−H bond scission. This was further supported by its ^{1}H NMR spectrum, which shows a singlet resonance at $\delta = -18.85$ ppm attributable to a hydride ligand, while the inequivalence of two pyridine rings is evident in the aromatic region. The incorporation of one equivalent of the oxime to the trinuclear framework and the presence of nine carbonyl ligands were confirmed by its microanalysis and FAB MS.

The structure proposed for **3**, and its role as an intermediate in the formation of **1** and **2** from $[Ru_3(CO)_{12}]$, were further corroborated by treating **3** with one equivalent of the oxime in THF at reflux temperature. This reaction led to complexes **1** and **2**, along with a small amount of $[Ru_3(CO)_{12}]$.

To the best of our knowledge, **1** and **3** are the first ruthenium cluster complexes containing oximate ligands. Some diruthenium(I) complexes structurally related to **2**, namely $[Ru_2(\mu,\eta^2\text{-ONCR}^1\text{R}^2\text{-}O,N)_2(CO)_4L_2]$ (L = intact oxime or other neutral two-electron donor ligands), have been reported.[10] It has also been reported that the reaction of $[Ru_3(CO)_{12}]$ with 1-nitrous-2-naphthol gives a triruthenium cluster structurally related to complex **1**, which also contains two NO bridges.[11]

The triosmium acetonitrile complex $[Os_3(CO)_{10}(MeCN)_2]$[12] reacts with Hdpko in THF at room temperature to give the monohydrido derivative $[Os_3(\mu\text{-H})(\mu,\eta^3\text{-dpko-}N,N,O)(CO)_9]$ (**4**; Scheme 2). The structure of this compound was established by X-ray diffraction methods (Figure 3, Table 3). The cluster consists of a nearly equilateral triangle of Os atoms in which two metal atoms are attached to a dpko ligand in the same way as that found previously for compounds **1** and **2**. A hydride ligand spans the same Os−Os edge as the oximate NO fragment. The cluster shell is completed by nine CO ligands. Therefore, the cluster is a closed-shell, 48-electron trinuclear species.[8] The spectroscopic data of **4** are similar to those of the ruthenium complex **3**, indicating that both compounds are isostructural.

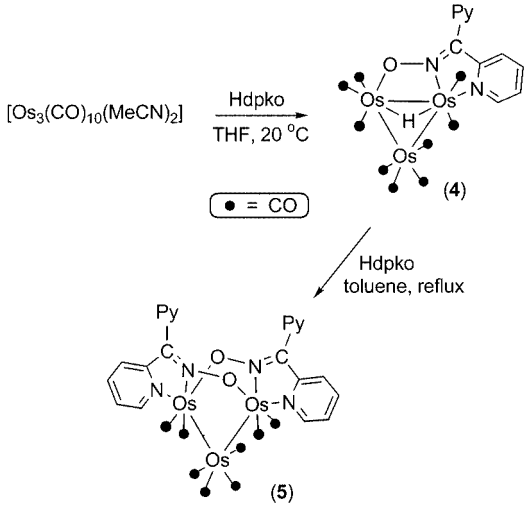

Scheme 2. Synthesis of compounds **4** and **5**

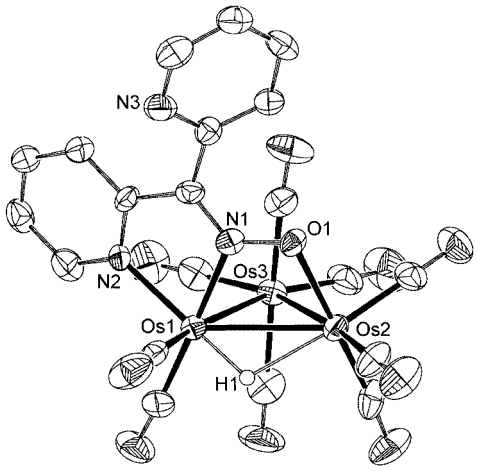

Figure 3. Molecular structure of compound **4** (50% probability level ellipsoids); H atoms (except the hydride) omitted for clarity

Table 3. Selected interatomic distances (Å) in complex **4**

Os(1)−Os(2)	2.861(5)	Os(1)−Os(3)	2.876(1)
Os(2)−Os(3)	2.855(2)	Os(1)−N(1)	2.062(9)
Os(1)−N(2)	2.078(9)	Os(2)−O(1)	2.170(7)
N(1)−O(1)	1.31(1)		

Therefore, the oxime Hdpko reacts with the triruthenium bis(acetonitrile) cluster in the same way as its triosmium analogue, giving isostructural products. However, this is not always the case for other ligands, such as bis(2-pyridyl)-amine,[13] 2-amino-7,8-benzoquinoline,[14] or 2,2′-diamino-1,1′-binaphthalene.[15]

Bearing in mind that the triruthenium complex **3** is an intermediate in the formation of **1**, we reasoned that complex **4** could be a suitable precursor of a triosmium cluster isostructural with complex **1**. Indeed, treatment of complex **4** with Hdpko in toluene at reflux temperature allowed the isolation of $[Os_3(\mu,\eta^3\text{-dpko-}N,N,O)_2(CO)_8]$ (**5**). The structure depicted for this complex in Scheme 2, which is similar to that of the triruthenium complex **1**, was determined by X-ray diffraction methods (Figure 4, Table 4). Accordingly, its IR and NMR spectroscopic data are also similar to those of complex **1**.

Very few triosmium clusters containing oximate ligands have been reported prior to this work. They contain oximate fragments that span two metal atoms through the N and O atoms.[4,5] During the preparation of this manuscript, some triosmium clusters related to compounds **4** and **5**, derived from diphenyl ketone oxime and phenyl (2-pyridyl) ketone oxime, have been reported.[6]

DNA-Cleavage Ability of the Oximate Complexes

Although most metal complex-mediated DNA cleavage reactions use mononuclear complexes as promoters,[16,17] a few interesting results have been reported using bi-[18] and trinuclear[19] complexes. Prompted by the fact that prior to

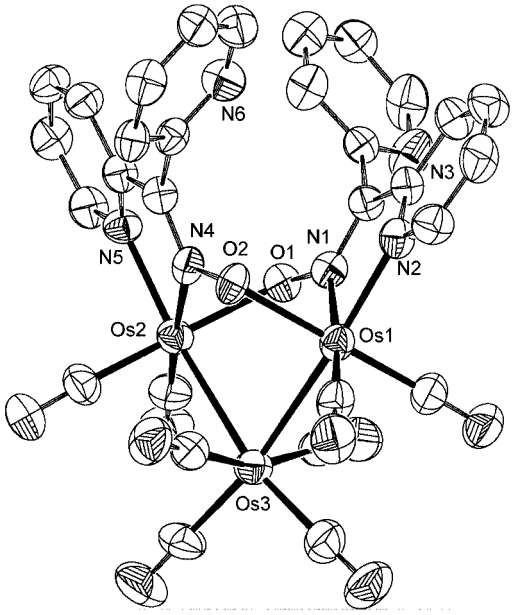

Figure 4. Molecular structure of compound **5** (50% probability level ellipsoids); H atoms omitted for clarity

Table 4. Selected interatomic distances (Å) in complex **5**

Os(1)−Os(2)	3.5903(5)	Os(1)−Os(3)	2.8318(6)
Os(2)−Os(3)	2.8274(5)	Os(1)−N(1)	2.125(7)
Os(1)−N(2)	2.130(7)	Os(2)−N(4)	2.145(8)
Os(2)−N(5)	2.148(7)	Os(1)−O(2)	2.130(6)
Os(2)−O(1)	2.124(6)	N(1)−O(1)	1.359(9)
N(4)−O(2)	1.346(9)		

this work no metal complexes of oximes had been studied as DNA cleaving agents, the ruthenium and osmium oximate complexes **1**−**5** were tested by studying the nicking of supercoiled circular φ*X174* RFI DNA (form I; 50 μM/base pair) into relaxed circular DNA (form II).

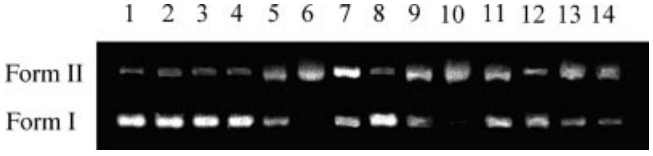

Figure 5. Electrophoresis separation of supercoiled circular φ*X174* RFI DNA (form I) and relaxed circular DNA (form II) after treatment of form I DNA with the ruthenium complexes **1**−**3**; lanes 1, 4, 8, 12 were run in the dark, the remaining ones involved UV light irradiation; lane 1, DNA alone (dark, pH = 7.0); lane 2, DNA alone (pH = 7.0); lane 3, DNA alone (pH = 5.0); lane 4, **1** (1000 μM, pH = 7.0, dark); lane 5, **1** (1000 μM, pH = 7.0); lane 6, **1** (1000 μM, pH = 5.0); lane 7, **1** (500 nM, pH = 5.0); lane 8, **2** (1000 μM, pH = 7.0, dark); lane 9, **2** (1000 μM, pH = 7.0); lane 10, **2** (1000 μM, pH = 5.0); lane 11, **2** (1.0 μM, pH = 5.0); lane 12, **3** (1000 μM, pH = 7.0, dark); lane 13, **3** (1000 μM, pH = 7.0); lane 14, **3** (1000 μM, pH = 5.0)

Figure 5 shows the results obtained with the ruthenium complexes. After UV irradiation of complexes **1**−**3** (1000 μM) and form I DNA, in pH 7.0 buffer for 8.0 h, ratios of (form II)/(form I) of 1.78, 1.63 and 2.57 were found (see lanes 5, 9, and 13). The cleaving ability of **1** and **2** was found to be pH dependent and is greater under slightly acidic conditions, cleaving DNA at pH 5.0 at concentrations of 500 nM (**1**) and 1.0 μM (**2**), with ratios of (form II)/(form I) of 1.27 and 1.08, respectively (lanes 7 and 11).

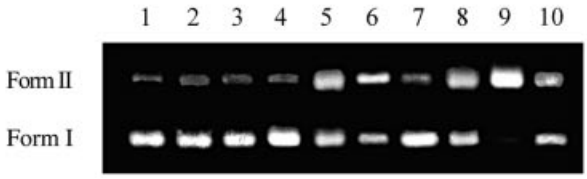

Figure 6. Electrophoresis separation of supercoiled circular φ*X174* RFI DNA (form I) and relaxed circular DNA (form II) after treatment of form I DNA with the osmium complexes **4** and **5**; lanes 1, 4, 7 were run in the dark, the remaining ones involved UV light irradiation; lane 1, DNA alone (dark, pH = 7.0); lane 2, DNA alone (pH = 7.0); lane 3, DNA alone (pH = 5.0); lane 4, **4** (1000 μM, pH = 7.0, dark); lane 5, **4** (1000 μM, pH = 7.0); lane 6, **4** (1000 μM, pH = 5.0); lane 7, **5** (1000 μM, pH = 7.0, dark); lane 8, **5** (1000 μM, pH = 7.0); lane 9, **5** (1000 μM, pH = 5.0); lane 10, **5** (1.0 μM, pH = 5.0)

For the osmium oximate complexes **4** and **5** (Figure 6), it was found that they can also cleave DNA upon UV activation. The ratios of (form II)/(form I) were 1.13 and 1.44 for **4** and **5** (1000 μM), respectively, in pH 7.0 buffer (see lanes 5 and 8). Complex **5** also cleaved DNA at pH 5.0 in concentrations of 1.0 μM to give a (form II)/(form I) ratio of 1.04 (see lane 10).

A comparison of the cleavage activity of the pairs of isostructural clusters **1**, **5** and **3**, **4** indicates that the ruthenium clusters (**1** and **3**) are more active than the osmium ones (**4** and **5**). In addition, the binuclear complex **2** is less active than the trinuclear ones **1** and **3**.

Although the cleaving ability of the Ru cluster complexes **1** and **3** is higher than that reported for other triruthenium carbonyl clusters,[19c] their activity is very low when compared to that of many mono- and binuclear compounds previously studied.[17,18] The high complex concentrations needed (millimolar range), along with long incubation times (8 h) and UV activation, hamper the use of these complexes for experiments in vivo.

Concluding Remarks

By using the oxime Hdpko as a ligand precursor, we have prepared one diruthenium, two triruthenium and two triosmium carbonyl complexes, all containing the oximate ligand dpko η^3-coordinated to two metal atoms through the N and O atoms of the oximate fragment and the N atom of the pyridyl group. Compounds **1** and **3** are the first ruthenium cluster complexes derived from oximes.

The first DNA cleaving studies using oximate metal complexes are described. Unfortunately, the observed activity is very low when compared to those of many mono- and binuclear compounds previously studied.

Experimental Section

General Synthetic and Characterization Data: Solvents were dried over sodium diphenyl ketyl (THF, Et_2O, hydrocarbons) or CaH_2 (dichloromethane) and distilled under nitrogen prior to use. The reactions were carried out under nitrogen, using Schlenk-vacuum line techniques, and were routinely monitored by solution IR spectroscopy (carbonyl stretching region) and spot TLC (silica gel). $[Os_3(CO)_{10}(MeCN)_2]$ was prepared as described previously;[12] the remaining reagents were purchased from commercial suppliers. IR: Perkin−Elmer Paragon 1000 FT. NMR: Bruker AC-200 and DPX-300, room temperature, TMS as internal standard. Microanalyses: Perkin−Elmer 2400. MS: VG Autospec double-focussing mass spectrometer operating in the FAB+ mode; ions were produced with a standard Cs^+ gun at ca. 30 kV; 3-nitrobenzyl alcohol (NBA) was used as matrix; data given refer to the most abundant molecular ion isotopomer.

$[Ru_3(\mu,\eta^3$-dpko-*N,N,O*$)_2(CO)_8]$ (1) and $[Ru_2(\mu,\eta^3$-dpko-*N,N,O*$)_2(CO)_4]$ (2): A solution of $[Ru_3(CO)_{12}]$ (104 mg, 0.163 mmol) and Hdpko (66 mg, 0.331 mmol) in THF (20 mL) was heated under reflux for 20 min. The color changed from orange to black. The solvent was concentrated under reduced pressure to ca. 2 mL and transferred onto TLC silica plates. Dichloromethane/THF (95:5) eluted four bands. The first two were very weak and were discarded. The third (orange) and fourth (pink) bands afforded compounds **1** (21 mg, 14%) and **2** (14 mg, 12%), respectively. A black residue remained uneluted at the base line.
1: FAB+ MS: *m/z* = 925 [M^+]. $C_{30}H_{16}N_6O_{10}Ru_3$ (923.74): calcd. C 39.01, H 1.75, N 9.09; found C 38.78, H 1.85, N 8.92. IR (CH_2Cl_2): ν(CO) = 2069 (m), 2007 (vs), 1990 (m), 1935 (w) cm^{-1}. ^1H NMR ([D_6]acetone): δ = 8.84 (ddd, *J* = 5.4, 1.7, 0.8 Hz, 1 H), 8.42 (ddd, *J* = 4.8, 1.7, 0.8 Hz, 1 H), 8.00 (td, *J* = 8.0, 1.7 Hz, 1 H), 7.54 (ddd, *J* = 8.0, 5.4, 1.1 Hz, 1 H), 7.52 (td, *J* = 7.7, 1.7 Hz, 1 H), 7.26 (ddd, *J* = 7.7, 4.8, 1.1 Hz, 1 H), 7.21 (ddd, *J* = 8.0, 1.1, 0.8 Hz, 1 H), 7.05 (ddd, *J* = 7.7, 1.1, 0.8 Hz, 1 H) ppm. $^{13}C\{^1H\}$ NMR (DEPT, CD_2Cl_2): δ = 206.1, 206.0, 202.6, 194.0 (COs); 160.3 (*C*=N); 156.2 (C_{ipso}), 152.3 (*C*H), 150.3 (C_{ipso}), 149.8 (*C*H), 137.8 (*C*H), 136.1 (*C*H), 126.4 (*C*H), 124.8 (*C*H), 123.9 (*C*H), 123.6 (*C*H) ppm.
2: FAB+ MS: *m/z* = 712 [M^+]. $C_{26}H_{16}N_6O_6Ru_2$ (710.59): calcd. C 43.94, H 2.27, N 11.83; found C 43.83, H 2.42, N 11.74. IR (CH_2Cl_2): ν(CO) = 2018 (vs), 1971 (w), 1943 (s) cm^{-1}. ^1H NMR ([D_6]acetone): δ = 9.04 (ddd, *J* = 5.2, 1.6, 0.8 Hz, 1 H), 8.65 (dt, *J* = 4.8, 1.6 Hz, 1 H), 7.91 (td, *J* = 8.3, 1.6 Hz, 1 H), 7.79−7.73 (m, 3 H), 7.47 (ddd, *J* = 7.6, 5.2, 1.6 Hz, 1 H), 7.34−7.30 (m, 1 H) ppm. $^{13}C\{^1H\}$ NMR (DEPT, CD_2Cl_2): δ = 211.9, 203.9 (COs); 155.7 (*C*=N); 153.7 (*C*H), 153.3 (C_{ipso}), 149.8 (*C*H), 149.0 (C_{ipso}), 137.5 (*C*H), 136.6 (*C*H), 127.3 (*C*H), 124.3 (*C*H), 124.2 (*C*H), 124.1 (*C*H) ppm.

$[Ru_3(\mu$-H$)(\mu,\eta^3$-dpko-*N,N,O*$)(CO)_9]$ (3): A solution of Me_3NO (40 mg, 0.533 mmol) in acetonitrile (10 mL) was slowly added to a solution of $[Ru_3(CO)_{12}]$ (150 mg, 0.235 mmol) in dichloromethane/acetonitrile (10:1, 20 mL) at −78 °C. Once the formation of $[Ru_3(CO)_{10}(MeCN)_2]$ was achieved (IR monitoring), Hdpko (51 mg, 0.256 mmol) was added and the solution was allowed to warm up to room temperature. Solvents were removed under reduced pressure and the residue was redissolved in THF (25 mL), whereupon the color changed from brown to black. The solvent was removed under reduced pressure, the residue was dissolved in ca. 1 mL of toluene and this solution was placed onto a silica gel column (2 × 8 cm) packed in hexanes. Elution with hexanes afforded some unchanged $[Ru_3(CO)_{12}]$. Elution with dichloromethane afforded complex **3** (40 mg, 23%). A black residue remained uneluted at the top of the column. FAB+ MS: *m/z* = 756 [M^+]. $C_{20}H_9N_3O_{10}Ru_3$ (754.55): calcd. C 31.84, H 1.20, N 5.57; found C 31.78, H 1.35, N 5.52. IR (CH_2Cl_2): ν(CO) = 2087 (m), 2047 (s), 2021 (vs), 2000 (s), 1978 (sh), 1959 (sh) cm^{-1}. ^1H NMR ($CDCl_3$): δ = 8.75 (d, *J* = 5.6 Hz, 1 H), 8.72 (dd, *J* = 5.2, 1.2 Hz, 1 H), 8.17 (br. d, *J* = 8.8 Hz, 1 H), 8.11 (d, *J* = 7.8 Hz, 1 H), 7.85 (td, *J* = 7.8, 1.6 Hz, 1 H), 7.71 (td, *J* = 8.8, 1.6 Hz, 1 H), 7.35 (td, *J* = 5.2, 1.2 Hz, 1 H), 7.20 (td, *J* = 5.2, 1.2 Hz, 1 H), −18.88 (s, μ-H) ppm.

$[Os_3(\mu$-H$)(\mu,\eta^3$-dpko-*N,N,O*$)(CO)_9]$ (4): Hdpko (85 mg, 0.427 mmol) was added to a solution of $[Os_3(CO)_{10}(MeCN)_2]$ (270 mg, 0.290 mmol) in THF (25 mL). The solution was stirred at room temperature for 2 h. The color changed from lemon yellow to red. The solvent was removed under reduced pressure, the residue was dissolved in ca. 2 mL of toluene and this solution was placed onto a silica gel column (2 × 10 cm) packed in hexanes. Elution with hexanes afforded some $[Os_3(CO)_{12}]$. Elution with hexanes/dichloromethane (1:1) afforded two bands. The first band (blue) was very weak and was not investigated. The second band (red) afforded complex **4** (125 mg, 42%). FAB+ MS: *m/z* = 1023 [M^+]. $C_{20}H_9N_3O_{10}Os_3$ (1021.90): calcd. C 23.51, H 0.89, N 4.11; found C 23.62, H 0.94, N 4.02. IR (CH_2Cl_2): ν(CO) = 2091 (m), 2051 (m), 2014 (vs), 1994 (m), 1964 (w), 1945 (w) cm^{-1}. ^1H NMR (CD_2Cl_2): δ = 9.04 (br. d, *J* = 5.9 Hz, 1 H), 8.73 (ddd, *J* = 4.7, 1.6, 0.8 Hz, 1 H), 8.40 (br. d, *J* = 8.4 Hz, 1 H), 8.12 (dt, *J* = 7.7, 1.2 Hz, 1 H), 7.87 (td, *J* = 7.7, 1.8 Hz, 1 H), 7.82 (ddd, *J* = 8.4, 7.7, 1.2 Hz, 1 H), 7.40 (ddd, *J* = 7.5, 4.7, 1.2 Hz, 1 H), 7.30 (ddd, *J* = 7.5, 5.9, 1.2 Hz, 1 H), −18.14 (s, μ-H) ppm. $^{13}C\{^1H\}$ NMR (DEPT, CD_2Cl_2): δ = 187.7, 186.7, 184.4, 181.0, 179.9, 177.8, 177.7, 175.0, 168.4 (COs); 154.8 (*C*=N); 154.7 (*C*H), 153.7 (C_{ipso}), 149.3 (*C*H), 148.2 (C_{ipso}), 136.7 (*C*H), 136.5 (*C*H), 127.6 (*C*H), 126.0 (*C*H), 124.6 (*C*H), 124.4 (*C*H) ppm.

$[Os_3(\mu,\eta^3$-dpko-*N,N,O*$)_2(CO)_8]$ (5): A solution of Hdpko (16 mg, 0.080 mmol) and complex **4** (80 mg, 0.078 mmol) in toluene (10 mL) was heated to reflux temperature for 75 min. The color changed from red to black. The solvent was partially removed under reduced pressure (to ca. 2 mL) and this solution was placed onto a silica gel column (2 × 10 cm) packed in hexanes. Elution with hexanes afforded some $[Os_3(CO)_{12}]$. Elution with hexanes/dichloromethane (1:2) afforded two weak bands, which were not investigated. Dichloromethane/THF (20:1) eluted a red band, which afforded complex **5** (18 mg, 19%). A black residue remained uneluted at the top of the column. FAB+ MS: *m/z* = 1192 [M^+]. $C_{30}H_{16}N_6O_{10}Os_3$ (1190.70): calcd. C 30.25, H 1.35, N 7.06; found C 30.42, H 1.42, N 7.06. IR (CH_2Cl_2): ν(CO) = 2071 (m), 1993 (vs), 1921 (m) cm^{-1}. ^1H NMR (CD_2Cl_2): δ = 8.73 (dd, *J* = 4.8, 0.8 Hz, 1 H), 8.33 (dd, *J* = 4.8, 0.8 Hz, 1 H), 7.74 (td, *J* = 8.0, 1.6 Hz, 1 H), 7.45 (td, *J* = 8.0, 2.0 Hz, 1 H), 7.24−7.06 (m, 4 H) ppm.

X-ray Diffraction Studies: Suitable crystals of **1**·C_6H_{14}, **2** and **5**·CH_2Cl_2 were obtained by slow diffusion of hexanes into dichloromethane solutions of the appropriate complexes. Crystals of **4** were obtained by slow diffusion of pentane into a solution of the complex in diethyl ether. Diffraction data for **1**·C_6H_{14} and **5**·CH_2Cl_2 were collected on a Nonius Kappa-CCD diffractometer equipped with a 95-mm CCD camera on a κ-goniostat, using graphite-monochromated Cu-K_α radiation. Diffraction data for **2** and **4** were collected on a Nonius CAD-4 diffractometer, with the ω-2θ scan technique and a variable scan rate, using graphite-monochromated Mo-K_α radiation, applying Lorentz and polarization corrections, and reducing the data to F_o^2 values. All structures were solved by Patterson interpretation using the program DIRDIF-96.[20] Absorption corrections were applied using XABS2[21] (**1**·C_6H_{14}, **2**, and

Table 5. Crystal, measurement, and refinement data for **1**·C_6H_{14}, **2**, **4**, and **5**·CH_2Cl_2

	1·C_6H_{14}	**2**	**4**	**5**·CH_2Cl_2
Empirical formula	$C_{30}H_{16}N_6O_{10}Ru_3$·$C_6H_{14}$	$C_{26}H_{16}N_6O_6Ru_2$	$C_{20}H_9N_3O_{10}Os_3$	$C_{30}H_{16}N_6O_{10}Os_3$·$CH_2Cl_2$
Formula mass	1009.87	710.59	1021.90	1276.01
Cryst. system	triclinic	monoclinic	monoclinic	triclinic
Space group	$P\bar{1}$	$P2_1/c$	$P2_1/a$	$P\bar{1}$
a, Å	10.6768(3)	9.029(2)	18.92(3)	10.8194(4)
b, Å	12.4667(4)	21.231(7)	7.566(2)	12.4036(4)
c, Å	15.6330(6)	13.43(2)	18.95(1)	15.4080(6)
α, deg	83.596(3)	90	90	85.049(2)
β, deg	79.614(2)	92.31(6)	120.05(7)	80.843(2)
γ, deg	72.495(2)	90	90	71.770(2)
V, Å^3	1948.3(1)	2573(4)	2349(4)	1937.4(1)
Z	2	4	4	2
F(000)	1000	1400	1832	1176
D_{calcd}, g cm^{-3}	1.721	1.835	2.889	2.187
Radiation (λ, Å)	Cu-K_α (1.54180)	Mo-K_α (0.71073)	Mo-K_α (0.71073)	Cu-K_α (1.54180)
μ, mm^{-1}	9.838	1.229	16.246	19.960
Cryst size, mm	0.33 × 0.20 × 0.13	0.33 × 0.10 × 0.10	0.27 × 0.10 × 0.07	0.17 × 0.07 × 0.07
Temp., K	200(2)	293(2)	293(2)	200(2)
θ limits, deg	2.88 to 69.76	1.80 to 25.98	1.24 to 25.98	2.91 to 69.93
Min/max *h*, *k*, *l*	−12/12, −14/15, −13/18	−11/0, −26/0, −16/16	−23/0, −9/0, −20/23	−12/13, −14/15, 0/18
No. of collected rflns.	9338	5361	4764	22303
No. of unique rflns. (R_{int})	6866 (0.0525)	5037 (0.0280)	4608 (0.0415)	7242 (0.0783)
No. of rflns. with $I > 2\sigma(I)$	6121	3399	3415	5680
Absorption correction	XABS2	XABS2	XABS2	SORTAV
Max/min transmission	0.278/0.141	0.884/0.863	0.321/0.156	1.249/0.744
No. of restraints/params.	83/515	0/361	0/326	0/496
GOF (on F^2)	1.106	1.015	1.030	0.962
Final *R*1 [on *F*, $I > 2\sigma(I)$]	0.0630	0.0317	0.0384	0.0481
Final *wR*2 (on F^2, all data)	0.2319	0.0884	0.1102	0.1291
Max/min residuals, e·Å^{-3}	1.266/−1.487	0.617/−0.554	1.974/−2.404	1.986/−1.708

4) or SORTAV[22] (**5**·CH_2Cl_2). Isotropic and full-matrix anisotropic least-squares refinements were carried out using SHELXL-97.[23] All non H atoms were refined anisotropically. Hydrogen atom positions were geometrically calculated and refined riding on their parent atoms, except the hydride H atom of **4**, which was located by Fourier difference maps. The disordered solvent molecule of **1**·C_6H_{14} was treated with a mixture of constraints and restraints as described elsewhere.[24] The solvent molecule of **5**·CH_2Cl_2 was found disordered over two positions, with partial occupancies of 0.5. The molecular plots were made with the EUCLID program package.[25] The WINGX program system[26] was used thorough the structure determinations. Selected crystal, measurement, and refinement data for the four X-ray structures are given in Table 5. CCDC-182375 (**1**·C_6H_{14}), -182376 (**2**), -203169 (**4**) and -203170 (**5**·CH_2Cl_2) contain the supplementary crystallographic data for this paper. These data can be obtained free of charge at www.ccdc.cam.ac.uk/conts/retrieving.html [or from the Cambridge Crystallographic Data Centre, 12, Union Road, Cambridge CB2 1EZ, UK; Fax: (internat.) +44-1223/336-033; E-mail: deposit@ccdc.cam.ac.uk].

DNA-Cleavage Experiments: All reactions were carried out in oven-dried (120 °C) or autoclaved glassware and eppendorf tubes. Supercoiled circular φ*X174* RFI DNA (molecular weight 3.50 × 10^6, 5386 base pairs in length) was purchased from New England Biolabs Co. The remaining reagents were also purchased from commercial suppliers. Photolytic experiments were carried out at 37 °C, using a medium pressure mercury lamp (350 nm, 32-W). The NIH 1.60 image program, provided by Dr. R. Wayne of National Institutes of Health, U. S. A., was used for the quantitative analysis of DNA cleavage.

In a typical experiment, a reaction mixture (10 μL) containing supercoiled circular φ*X174* RFI DNA stock solution (form I, 50 μM/base pair, 1.0 μL), an oximate complex (10 mM, 1.0 μL), and a phosphate buffer (0.10 M, 8.0 μL) was preincubated at 37 °C in a Pyrex vial and irradiated with UV light (350 nm, 32-W) under aerobic conditions for 8.0 h. After addition of the gel-loading buffer (0.25% bromophenol blue, 0.25% xylene cyanol, and 30% glycerol), the reaction mixture was loaded onto a 1% agarose gel with ethidium bromide staining. The electrophoresis tank was attached to a power supply at a constant current of about 100 mA). The gel was visualized by 312-nm UV transilluminator and photographed by an FB-PDC-34 camera. Quantification of DNA cleavage activity was performed by integration of the optical density of the spot as a function of the band area by use of a Microtek scanner and the NIH 1.60 image program.

Acknowledgments

This work has been supported by the Spanish MECD (grant PB98-1555 to J. A. C.), MCYT (grants BQU2000-2019 to S. G.-G. and BQU2002-2623 to J. A. C.), and Principado de Asturias (grant PR-01-GE-7 to V. R.), and by the Republic of China's National Science Council (to J. R. H.).

[1] A. Chakravorty, *Coord. Chem. Rev.* **1974**, *13*, 1−46.
[2] [2a] A. R. Middleton, J. R. Thornback, G. Wilkinson, *J. Chem. Soc., Dalton Trans.* **1980**, 174−179. [2b] T. Daniel, W. Knaup, M. Dziallas, H. Werner, *Chem. Ber.* **1993**, *126*, 1981−1993. [2c] H. Werner, T. Daniel, W. Knaup, O. Nürnberg, *J. Organomet. Chem.* **1993**, *462*, 309−318. [2d] R. Castarlenas, M. A. Es-

teruelas, E. Gutiérrez-Puebla, Y. Jean, A. Lledós, M. Martín, J. Tomás, *Organometallics* **1999**, *18*, 4296−4303.
[3] T. Carofiglio, S. Stella, C. Floriani, A. Chiesi-Villa, C. Guastini, *J. Chem. Soc., Dalton Trans.* **1989**, 1957−1962.
[4] A. J. Deeming, D. W. Owen, N. I. Powell, *J. Organomet. Chem.* **1990**, *398*, 299−310.
[5] M. H. Chao, S. Kumaresan, Y. S. Wen, S. C. Lin, J. R. Hwu, K.-L. Lu, *Organometallics* **2000**, *19*, 714−717.
[6] J. S. Y. Wong, W. T. Wong, *New J. Chem.* **2002**, *26*, 94−104.
[7] Hdpko has heretofore been used to prepare Ag,[11a] Cu,[11a,11b] Zn[11c] and Ni[11d] derivatives. [7a] S. O. Sommerer, B. L. Westcott, A. J. Jircitano, K. A. Abboud, *Inorg. Chim. Acta* **1995**, *238*, 149−153. [7b] M. A. S. Goher, F. A. Mautner, *Polyhedron* **1999**, *18*, 3425−3431. [7c] A. J. Stemmler, J. W. Kampf, V. L. Pecoraro, *Inorg. Chem.* **1995**, *34*, 2271−2272. [7d] G. Psomas, C. Dendrinou-Samara, M. Alexiou, A. Tsohos, C. P. Raptopoulou, A. Terzis, D. P. Kessissoglou, *Inorg. Chem.* **1998**, *37*, 6556−6557.
[8] D. M. P. Mingos, D. J. Wales, *Introduction to Cluster Chemistry*, Prentice-Hall International, Englewood Cliffs, NJ, **1990**.
[9] G. A. Foulds, B. F. G. Johnson, J. Lewis, *J. Organomet. Chem.* **1985**, *296*, 147−153.
[10] [10a] M. Langenbahn, H. Stoeckli-Evans, G. Süss-Fink, *J. Organomet. Chem.* **1990**, *397*, 347−358. [10b] M. Langenbahn, H. Stoeckli-Evans, G. Süss-Fink, *Helv. Chim. Acta* **1991**, *74*, 549−553.
[11] K. K. H. Lee, W. T. Wong, *J. Chem. Soc., Dalton Trans.* **1997**, 2987−2996.
[12] M. J. Nicholls, M. D. Vargas, *Inorg. Synth.* **1990**, *28*, 232−235.
[13] J. A. Cabeza, I. del Río, S. García-Granda, V. Riera, M. Suárez, *Organometallics* **2002**, *21*, 2540−2543.
[14] J. A. Cabeza, I. del Río, S. García-Granda, V. Riera, M. Suárez, *Organometallics* **2002**, *21*, 5055−5059.
[15] J. A. Cabeza, I. da Silva, I. del Río, S. García-Granda, V. Riera, M. G. Sánchez-Vega, *Organometallics* **2003**, *22*, 1519−1525.
[16] [16a] N. Farrell, in *Catalysis by Metal Complexes* (Eds.: R. Ugo, B. R. James), Kluwer Academic Publishers, Dordrecht, The Netherlands, **1989**, Vol. 11, p. 17. [16b] J. Kim, M. F. Sistare, P. J. Carter, H. H. Thorp, *Coord. Chem. Rev.* **1998**, *171*, 341−349. [16c] A. Sreedhara, J. D. Freed, J. A. Cowan, *J. Am. Chem. Soc.* **2000**, *122*, 8814−8824. [16d] G. Roelfes, M. E. Branum, W. Li, L. Que, B. L. Feringa, *J. Am. Chem. Soc.* **2000**, *122*, 11517−11518. [16e] S. Dhar, A. R. Chakravarty, *Inorg. Chem.* **2003**, *42*, 2483−2485.
[17] For recent reviews, see: [17a] G. Pratviel, J. Bernadou, B. Meunier, *Adv. Inorg. Chem.* **1997**, *45*, 251−312. [17b] B. Armitage, *Chem. Rev.* **1998**, *98*, 1171−1200. [17c] Z. Guo, P. J. Sadler, *Angew. Chem. Int. Ed.* **1999**, *38*, 1512−1531. [17d] K. E. Erkkila, D. T. Odom, J. K. Barton, *Chem. Rev.* **1999**, *99*, 2777−2796. [17e] G. Pratviel, J. Bernadou, B. Meunier, *Angew. Chem. Int. Ed. Engl.* **1995**, *34*, 746−769. [17f] S. J. Franklin, *Cur. Op. Chem. Biol.* **2001**, *5*, 201−208.
[18] [18a] F. O'Reilly, J. Kelly, A. Kirsch-De-Mesmaeker, *Chem. Commun.* **1996**, 1013−1014. [18b] M. E. Branum, L. Que, *J. Biol. Inorg. Chem.* **1999**, *4*, 593−600. [18c] M. E. Branum, A. K. Tipton, S. Zhu, L. Que, *J. Am. Chem. Soc.* **2001**, *123*, 1898−1904.
[19] [19a] K. J. Humphreys, K. D. Karlin, S. E. Rokita, *J. Am. Chem. Soc.* **2001**, *123*, 5588−5589. [19b] C. S. Allardyce, P. J. Dyson, *J. Cluster Sci.* **2001**, *12*, 563−569. [19c] J. R. Hwu, K.-L. Lu, S.-F. Yu, L.-J. Yu, S. Kumaresan, K.-J. Lin, S.-C. Tsay, *Photochem. Photobiol.* **2002**, *75*, 457−461. [19d] E. Rosenberg, F. Spada, K. Sugden, B. Martin, L. Milone, R. Gobetto, A. Viale, J. Fiedler, *J. Organomet. Chem.* **2003**, *668*, 51−58.
[20] P. T. Beurskens, G. Beurskens, W. P. Bosman, R. de Gelder, S. García-Granda, R. O. Gould, R. Israël, J. M. M. Smits, *The DIRDIF-96 Program System, Crystallography Laboratory*, University of Nijmegen, The Netherlands, **1996**.
[21] S. Parkin, B. Moezzi, H. Hope, *J. Appl. Cryst.* **1995**, *28*, 53−56.
[22] R. H. Blessing, *Acta Crystallogr., Sect. A* **1995**, *51*, 33−38.
[23] G. M. Sheldrick, *SHELXL-97, version 97−2*, University of Göttingen, Germany, **1997**.
[24] J. F. van der Maelen, *Cryst. Rev.* **1999**, *7*, 125−187.
[25] A. L. Spek, *The EUCLID Package*, in *Computational Crystallography* (Ed.: D. Sayre), Clarendon Press, Oxford, UK, **1982**, p. 528.
[26] L. J. Farrugia, *J. Appl. Crystallogr.* **1999**, *32*, 837−838.

Received June 4, 2003
Early View Article
Published Online October 10, 2003

